ORGANOMETALLICS

Formation of .eta.2-iminoacyl compounds by protonation of a ketenimine ligand in bis((trimethylsilyl)cyclopentadienyl) compounds of niobium. Molecular structures of [Nb(.eta.5-C5H4SiMe3)2Cl(.eta.2(C,N)-EtPhHCCNPh)]+BF4- and [Nb(.eta.5-C5H4SiMe3)2F(.eta.2(C,N)-Ph2HCCNPh)]+BF4-

Antonio Antinolo, Mariano Fajardo, Raquel Gil-Sanz, Carmen Lopez-Mardomingo, Partricia Martin-Villa, Antonio Otero, Marek M. Kubicki, Yves Mugnier, S. El Krami, and Y. Mourad

Organometallics, **1993**, 12 (2), 381-388• DOI: 10.1021/om00026a024 • Publication Date (Web): 01 May 2002

Organometallics **1993,** *12,* 381-388

Formation of η^2-Iminoacyl Compounds by Protonation of a Ketenimine Ligand in Bis((trimethylsilyl)cyclopentadienyl) Compounds of Niobium. Molecular Structures of $[Nb(\eta^5\text{-}C_5H_4SiMe_3)_2Cl(\eta^2(C,N)\text{-}EtPhHCCNPh)]^+BF_4^-$ and $[Nb(\eta^5\text{-}C_5H_4SiMe_3)_2F(\eta^2(C,N)\text{-}Ph_2HCCNPh)]^+BF_4^-$

Antonio Antiñolo,[†] Mariano Fajardo,[‡] Raquel Gil-Sanz,[‡]
Carmen López-Mardomingo,[‡] Patricia Martín-Villa,[‡] Antonio Otero,[*,†]
Marek M. Kubicki,[§] Yves Mugnier,[§] S. El Krami,[§] and Y. Mourad[§]

Departamento de Química Inorgánica, Orgánica y Bioquímica, Facultad de Químicas, Universidad de Castilla-La Mancha, 13071 Ciudad Real, Spain, Departamento de Química Inorgánica and Departamento de Química Orgánica, Campus Universitario, Universidad de Alcalá, 28871 Alcalá de Henares, Spain, and Laboratoire de Synthèse et d'Electrosynthèse Organometalliques associé au CNRS (URA 33), Faculté des Sciences, 6 Boulevard Gabriel, 21000 Dijon, France

Received June 11, 1992

$Nb(\eta^5\text{-}C_5H_4SiMe_3)_2X(\eta^2(C,N)\text{-}R^1R^2CCNR^3)$ (X = Cl, Br) reacts with 1 equiv of $HBF_4{\cdot}OEt_2$ to give in one step the η^2-iminoacyl complexes $[Nb(\eta^5\text{-}C_5H_4SiMe_3)_2X(\eta^2(C,N)\text{-}R^1R^2HCCNR^3]^+BF_4^-$ (**1**, X = Cl, $R^1 = R^2 = R^3 = C_6H_5$ (Ph); **2**, X = Br, $R^1 = R^2 = R^3$ = Ph; **3**, X = F, $R^1 = R^2 = R^3$ = Ph; **4**, X = Cl, $R^1 = R^3$ = Ph, $R^2 = C_2H_5$ (Et); **5**, X = Br, $R^1 = R^3$ = Ph, R^2 = Et; **6**, X = Cl, $R^1 = R^3$ = Ph, $R^2 = CH_3$ (Me); **7**, X = Br, $R^1 = R^3$ = Ph, R^2 = Me; **8**, X = Cl, $R^1 = R^2$ = Ph, R^3 = *p*-Br-C_6H_4; **9**, X = Br, $R^1 = R^2$ = Ph, R^3 = *p*-Br-C_6H_4) through protonation at the free terminus of the complexed ketenimine ligands. Complex **3** has also been isolated as both the N-outside and N-inside conformers in the three-step reaction (oxidation, F^- abstraction, and protonation processes) of $Nb(\eta^5\text{-}C_5H_4SiMe_3)_2(\eta^2(C,N)\text{-}Ph_2CCNPh)$ with 2 equiv of $HBF_4{\cdot}OEt_2$. The chemical (Na/Hg) and electrochemical one-electron reductions of complexes **1**–**9** yield the starting ketenimine complexes with the evolution of H_2. The structures of **3** and **4** were determined by single-crystal diffractometry. Compound **3** crystallizes in the monoclinic space group $P2_1/n$ with a = 11.004 (4) Å, b = 17.702 (5) Å, c = 18.679 (4) Å, β = 91.60 (2)°, Z = 4, V = 3637.3 Å^3, ρ_{calcd} = 1.358 g/mL, R = 0.051, and R_w = 0.058 based on 6832 reflections. Compound **4** crystallizes in the monoclinic space group $C2/c$ with a = 23.962 (8) Å, b = 21.408 (5) Å, c = 16.456 (3) Å, β = 123.30 (2)°, Z = 8, V = 7055.5 Å^3, ρ_{calcd} = 1.368 g/mL, R = 0.046, and R_w = 0.048 based on 5856 reflections. The molecular structures show a typical bent-metallocene geometry around the niobium atom with an η^2(C,N)-bonded iminoacyl ligand.

Introduction

Insertion reactions of isocyanides into transition-metal–carbon bonds to give iminoacyl groups are commonly encountered in organometallic chemistry.[1] For early transition metals the most extensive studies have been reported on the spectroscopic and structural properties of the group 4 metal η^2-iminoacyl derivatives.[2] In contrast, the study of analogous group 5 metal complexes has been much less thorough. Several years ago, Wilkinson et al.[3] reported the first tantalum iminoacyl complexes from the interactions of Me_xTaCl_{5-x} complexes with the appropriate isocyanides, and recently several related complexes containing the ancillary aryloxide ligand have also been described.[4] A structurally characterized (iminoacyl)-vanadocene complex has also been reported.[5] To date in the niobium chemistry only a few (iminoacyl)niobocene complexes, described by some of us,[6,7] have been reported. One of those was specifically prepared from a neutral

---

[†] Universidad de Castilla-La Mancha.

[‡] Universidad de Alcalá.

[§] Laboratoire de Synthèse et d'Electrosynthèse Organometalliques.

[1] (a) Singleton, E.; Oosthuizen, H. E. *Adv. Organomet. Chem.* **1983**, *22*, 209. (b) Treichel, P. M. *Adv. Organomet. Chem.* **1983**, *11*, 21. (c) Durfee, L. D.; Rothwell, I. A. *Chem. Rev.* **1988**, *88*, 1059.

[2] (a) Clark, R. J. H.; Stockwell, J. A.; Wilkins, J. D. *J. Chem. Soc., Dalton Trans.* **1976**, 120. (b) Lappert, M. F.; Luong Thi, N. T.; Milne, C. R. *J. Organomet. Chem.* **1979**, *174*, C35. (c) Wolczanski, P. T.; Bercaw, J. E. *J. Am. Chem. Soc.* **1979**, *101*, 6450. (d) Andersen, R. A. *Inorg. Chem.* **1979**, *18*, 2928. (e) De Boer, E. J. M.; Teuben, J. H. *J. Organomet. Chem.* **1979**, *166*, 193. (f) Bolhuis, F.; De Boer, E. J. M.; Teuben, J. H. *J. Organomet. Chem.* **1979**, *170*, 299. (g) Dormond, A.; Dahchour, A. *J. Organomet. Chem.* **1980**, *193*, 321. (h) Klei, E.; Telgen, J. H.; Teuben, J. H. *J. Organomet. Chem.* **1981**, *209*, 297. (i) Reger, D. L.; Tarquini, M. K.; Lebioda, L. *Organometallics* **1983**, *2*, 1763. (j) Fandos, R.; Meetsma, A.; Teuben, J. H. *Organometallics* **1991**, *10*, 2665. (k) Martin, B. D.; Matchett, S. A.; Norton, J. R.; Anderson, O. P. *J. Am. Chem. Soc.* **1985**, *107*, 7952. (l) Lubben, T. V.; Plössl, K.; Norton, J. R.; Miller, M. M.; Anderson, O. P. *Organometallics* **1992**, *11*, 122.

[3] Chiu, K. W.; Jones, R. A.; Wilkinson, G.; Galas, A. M. R.; Hursthouse, M. B. *J. Chem. Soc., Dalton Trans* **1981**, 2088.

[4] (a) Chamberlain, L. R.; Durfee, L. D.; Fanwick, P. E.; Kobriger, L.; Latesky, S. L.; McMullen, A. K.; Rothwell, I. P.; Folting, K.; Huffman, J. C.; Streib, W. E.; Wang, R. *J. Am. Chem. Soc.* **1987**, *109*, 390. (b) McMullen, A. K.; Rothwell, I. P.; Huffman, J. C. *J. Am. Chem. Soc.* **1985**, *107*, 1072. (c) Latesky, S. L.; McMullen, A. K.; Niccolai, G. P.; Rothwell, I. P.; Huffman, J. C. *Organometallics* **1985**, *4*, 1896. (d) Chamberlain, L. R.; Rothwell, I. P.; Huffmann, J. C. *J. Chem. Soc., Chem. Commun.* **1986**, 1203.

[5] Carrier, A. M.; Davidson, J. G.; Barefield, E. K.; Van Derveer, D. G. *Organometallics* **1987**, *6*, 454.

[6] Martínez de Ilarduya, J. M.; Otero, A.; Royo, P. *J. Organomet. Chem.* **1988**, *340*, 187.

[7] Antiñolo, A.; Fajardo, M.; López-Mardomingo, C.; Otero, A.; Mourad, Y.; Mugnier, Y.; Sanz-Aparicio, J.; Fonseca, I.; Florencio, F. *Organometallics* **1990**, *9*, 1919.

0276-7333/93/2312-0381$04.00/0

(ketenimine)niobium(IV) complex by means of a two-step process, as illustrated in eq 1.

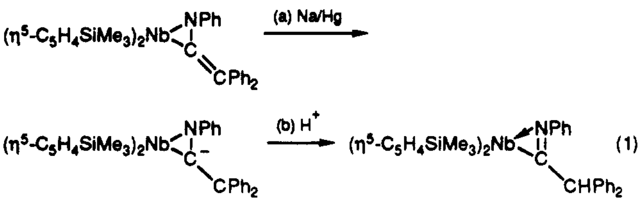

In order to explore the new reactivity of our (ketenimine)niobocene complexes,[7] we have decided to try an easy route for the synthesis of η^2-iminoacyl complexes based on electrophilic attack at the free terminus of the complexed ketenimine ligands, which has been successful in the isolation of acyl derivatives from (ketene)niobocene complexes.[8] This paper will focus on the preparation and structural details of cationic (η^2-iminoacyl)niobocene complexes.[9] Electrochemical data are also discussed.

Results and Discussion

The reactions of several (ketenimine)niobocene complexes with tetrafluoroboric acid were investigated. The standard reaction procedure involved addition of 1 equiv of $HBF_4{\cdot}OEt_2$ to a red solution of $Nb(\eta^5\text{-}C_5H_4SiMe_3)_2X(\eta^2(C,N)\text{-}R^1R^2CCNR^3)$ in THF at room temperature to give, after stirring for 1 h, white solids corresponding to the η^2-iminoacyl complexes $[Nb(\eta^5\text{-}C_5H_4SiMe_3)_2X(\eta^2(C,N)\text{-}R^1R^2HCCNR^3)]^+BF_4^-$ (eq 2).

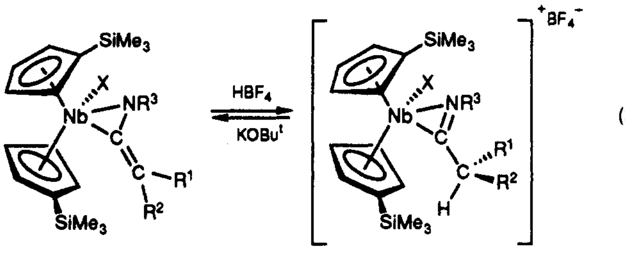

(2)

1–9

1, X = Cl, $R^1 = R^2 = R^3 = C_6H_5$(Ph); **2**, X = Br, $R^1 = R^2 = R^3$ = Ph; **3**, X = F, $R^1 = R^2 = R^3$ = Ph; **4**, X = Cl, $R^1 = R^3$ = Ph, $R^2 = C_2H_5$ (Et); **5**, X = Br, $R^1 = R^3$ = Ph, R^2 = Et; **6**, X = Cl, $R^1 = R^3$ = Ph, R^2 = (Me); **7**, X = Br, $R^1 = R^3$ = Ph, R^2 = Me; **8**, X = Cl, $R^1 = R^2$ = Ph, R^3 = *p*-Br-C_6H_4; **9**, X = Br, $R^1 = R^2$ = Ph, R^3 = *p*-Br-C_6H_4

The crude products were isolated as air-stable white solids and were purified by crystallization (CH_2Cl_2/hexane) and characterized by IR and NMR spectroscopy and analysis. These processes were reversible; thus, a facile H^+ abstraction from the iminoacyl ligand was observed when **1**–**9** were allowed to react with 1 equiv of KO^{t}Bu to give the starting ketenimine complexes.[10] Complex **3** can also be obtained by reaction of $Nb(\eta^5\text{-}C_5H_4SiMe_3)_2(\eta^2(C,N)\text{-}Ph_2CCNPh)$[7] with 2 equiv of $HBF_4{\cdot}OEt_2$. A brown solution of that complex in Et_2O reacts at room temperature with $HBF_4{\cdot}OEt_2$ to give instantaneously a white precipitate which was identificated as **3** by comparison with a genuine sample. We have observed[11] that the oxidation process of our (ketenimine)niobium(IV) compound with H^+ (from $HBF_4{\cdot}OEt_2$) in the molar ratio 1:1 gives the $Nb(\eta^5\text{-}C_5H_4SiMe_3)_2F(\eta^2(C,N)\text{-}Ph_2CCNPh)$ complex as the final product (eq 3). Thus, this compound could participate as an

$$NbCp'_2(\eta^2(C,N)\text{-}Ph_2CCNPh) + HBF_4{\cdot}OEt_2 \xrightarrow[H_2]{Et_2O}$$

$$\text{“}[NbCp'_2(\eta^2(C,N)\text{-}Ph_2CCNPh)]^{+}\text{”} \xrightarrow{F^- \text{ abstraction}}$$

$$NbCp'_2F(\eta^2(C,N)\text{-}Ph_2CCNPh) \quad (3)$$

$$Cp' = \eta^5\text{-}C_5H_4SiMe_3$$

intermediate in the formation of **3** through the protonation process of eq 2. Complex **3** has been isolated in this preparation as a mixture of two isomers, N-outside and N-inside; however, we have isolated the N-inside conformer

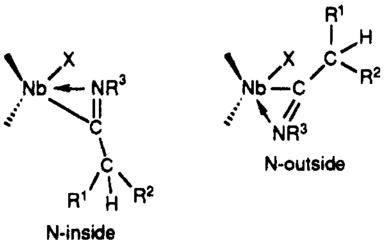

as the major product. The IR and NMR spectra of complexes **1**–**9** prove they contain the η^2-iminoacyl moiety. In our complexes the IR ν(C–N) absorption appears at ca. 1700 cm^{-1} and this value agrees with values previously reported for structurally characterized η^2-iminoacyl complexes. Structural characterization of two derivatives (vide infra) confirms our expectation. ^1H NMR spectra show resonances corresponding to both the cyclopentadienyl rings and the iminoacyl ligand. However, the most notable characteristic of the NMR spectra is the position in the ^{13}C NMR spectrum of the resonance for the η^2-CNR^3 carbon atom, which was found to resonate at ca. δ 215 ppm in accordance with data previously reported for η^2-iminoacyl complexes of early transition metals.[1-5] Both ^1H and ^{13}C NMR data indicated the presence of one of two (N-outside and N-inside) possible conformations in the complexes isolated via eq 2. Although it has been demonstrated[12] that the N- or O-outside isomer is the resulting initial kinetic iminoacyl or acyl product of the insertion reaction, most group 4 metal derivatives show the structure of the N- or O-inside isomer. The X-ray crystal structure determination has shown that complexes **3** and **4** have the ground-state structure N-inside with the bulky fragments away from the halogen atom. However, the IR and NMR data indicate complex **3**, prepared from $Nb(\eta^5\text{-}C_5H_4SiMe_3)_2(\eta^2(C,N)\text{-}Ph_2CCNPh)$ (see eq 3), crystallizes as a mixture of the two conformers. Appropriate workup allows the separation of both isomers. This behavior, as far as we know, has no precedence in the field

---

(8) (a) Bruno, J. W.; Fermin, M. C.; Halfon, S. E.; Schulte, G. K. *J. Am. Chem. Soc.* **1989**, *111*, 8738. (b) Antiñolo, A.; Otero, A.; Fajardo, M.; López-Mardomingo, C.; Lucas, D.; Mugnier, Y.; Lanfranchi, M.; Pellinghelli, M. A. *J. Organomet. Chem.* **1992**, *435*, 55.

(9) Some aspects of this work have been communicated: Antiñolo, A.; Fajardo, M.; López-Mardomingo, C.; Martín-Villa, P.; Otero, A.; Kubicki, M. M.; Mourad, Y.; Mugnier, Y. *Organometallics* **1991**, *10*, 3435.

(10) A similar procedure, the deprotonation of an α-proton of an acyl moiety, affords an efficient route to $\eta^2(C,O)$-ketene complexes: (a) Bristow, G. S.; Hitchcock, P. B.; Lappert, M. F. *J. Chem. Soc., Chem. Commun.* **1982**, 462. (b) Moore, E. J.; Straus, D. A.; Armantrout, J.; Santarsiero, B. D.; Grubbs, R. H.; Bercaw, J. E. *J. Am. Chem. Soc.* **1983**, *105*, 2068. (c) Straus, D. A.; Grubbs, R. H. *J. Am. Chem. Soc.* **1982**, *104*, 5499.

(11) Antiñolo, A.; Fajardo, M.; Gil-Sanz, R.; López-Mardomingo, C.; Otero, A., unpublished results.

(12) Erker, G. *Acc. Chem. Res.* **1984**, *17*, 103.

of the (iminoacyl)metallocenes of early transition metals. Ohtaki et al.[13] have recently reported the existence in solution of two isomers, S-outside and S-inside, from a (thioacyl)zirconocene complex. Also, NMR considerations for one α-zirconocenyl thioether have suggested the presence of a mixture of S-inside and S-outside isomers in solution.[14] In an elegant study on the electronic and geometrical structure of η^2-acyl complexes of group 4 metals, Hoffmann et al.[15] have pointed out that the directionality of the LUMO of d^0 Cp_2ML_2 systems favors a lateral approach of a ligand over a central one. Thus, the two possible modes of attack of the F^-, in the fluoride abstraction process, over either face of the complexed ketenimine ligand in the initial cationic species of Nb(V) (see eq 3), could probably explain our results:

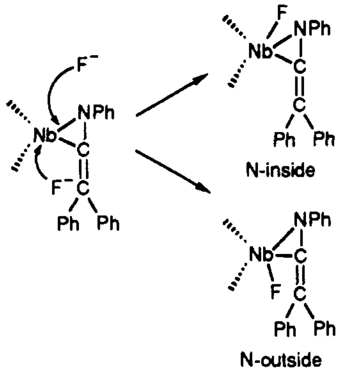

Obviously the third step, a protonation process to give the iminoacyl complex, will yield a mixture of the two isomers. This comment is in agreement with the following experimental result: we have also isolated a mixture of two isomers of $Nb(\eta^5\text{-}C_5H_4SiMe_3)_2F(\eta^2(C,N)\text{-}Ph_2CCNPh)$ when the reaction between $Nb(\eta^5\text{-}C_5H_4SiMe_3)_2(\eta^2(C,N)\text{-}Ph_2CCNPh)$ and $HBF_4 \cdot OEt_2$ was carried out in a 1:1 molar ratio.[11]

Reactivity of Niobium η^2-Iminoacyl Groups. In contrast to the chemistry of acyl complexes, studies on the reactivity of iminoacyl complexes of early transition metals have been scarcely undertaken. Illustrative examples of these are both intramolecular coupling (carbon–carbon double-bond formation) and hydrogenation processes to give enediamide[4c,d] and amide[16] functions, respectively. Our η^2-iminoacyl complexes **1**–**9** do not react with H_2 (1 atm), and we do not also observe any change on thermolysis (120 °C toluene solutions for several hours).

In order to gain more insight into the reactivity of the η^2-iminoacyl group in our complexes, we have tested both the electrochemical and chemical behavior toward the reduction processes.

Table I. Half-Wave Potentials (V) of Derivatives 1–9 from Polarography Referred to a Saturated Calomel Electrode (SCE)[a]

	wave		
derivatives	A	B	C_1
1	−0.95	−1.95	−2.40
2	−0.75		
	−0.65[b]	−1.57[b]	−2.41[b]
3	−1.01	−1.56	−2.40
	−1.18	−1.86	−2.40
4	−1.00		
5	−0.84		
6	−1.00		
	−0.90[b]	−1.82[b]	−2.55[b]
7	−0.75		
8	−0.85	−1.58	−2.43
9	−0.70	−1.65	−2.43

[a] All potentials are at room temperature unless otherwise noted. [b] At 50 °C.

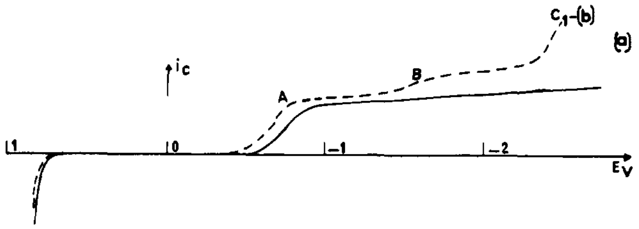

Figure 1. Polarogram of **2** in $THF\text{–}Bu_4NPF_6$ solution (average current; $t = 0.5$ s): (a) at room temperature; (b) at 50 °C.

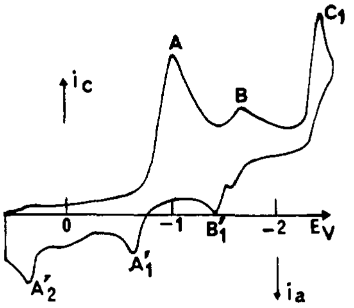

Figure 2. Cyclic voltammogram of **2** in $THF\text{–}Bu_4NPF_6$ solution at a platinum electrode (starting potential +0.6 V; sweep rate 0.2 V s^{-1}).

Electrochemical Behavior of η^2-Iminoacyl Complexes. In THF at a mercury electrode ($\tau = 0.5$ s) with 0.2 M tetrabutylammonium hexafluorophosphate as supporting electrolyte the polarograms of compounds **1**–**9** generally exhibit the three reduction waves A, B, and C_1 (see Table I). For complex **3**, where two conformers are present, the two waves A_1 and A_2 ($E_{1/2} = -1.01$ V and $E_{1/2} = -1.18$ V, respectively) are observed. Wave B, corresponding to the reduction of the ketenimine derivatives $Nb(\eta^5\text{-}C_5H_4SiMe_3)_2X(\eta^2(C,N)\text{-}R^1R^2CCNR^3)$, is observed for complexes **1**, **3**, **8**, and **9** at room temperature and at 50 °C for derivatives **2** and **6**. In the case of derivatives **4**, **5** and **7** the reduction wave was not observed even at 50 °C. We have previously shown that the corresponding ketenimine ligand was reduced at the potential of wave C_1.[7] Figure 1 shows, for example, the polarogram of complex **2** at both room temperature and 50 °C. In cyclic voltammetry at a platinum electrode, for all of the complexes, the peaks A, B, and C_1 appear no matter what the temperature. Figure 2 shows the cyclic voltammogram of **2** at room temperature; the height of peak B is smaller than that of peak A, and it decreases at low temperature. Inversion of the potential scan after peak C_1 produces the three oxidation peaks B'_1, A'_1, and A'_2 (a shoulder appears at −1.6 V). Figure 3 shows the thin-layer voltammogram of **2**, where the well-defined system B/B'_1 appears. Peaks A'_1 and A'_2 are observed when the potential scan is reversed after peak A. Electrolysis of the chloro and fluoro derivatives (**1**, **3**, **4**, **6**, and **8**) at the potential of wave A at

---

[13] Ando, W.; Ohtaki, T.; Suzuki, T.; Kabe, Y. *J. Am. Chem. Soc.* **1991**, *113*, 7782.

[14] Ward, A. S.; Mintz, E. A.; Ayers, M. R. *Organometallics* **1986**, *5*, 1585.

[15] Tatsumi, K.; Nakamura, A.; Hofmann, P.; Stauffert, P.; Hoffmann, R. *J. Am. Chem. Soc.* **1985**, *107*, 4440.

[16] Fromberg, W.; Erker, G. *J. Organomet. Chem.* **1985**, *280*, 340.

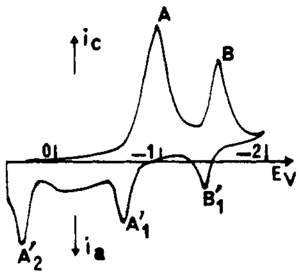

Figure 3. Thin-layer voltammogram of 2 in THF–Bu_4NPF_6 solution at a platinum electrode (starting potential +0.5 V; sweep rate 0.02 V s^{-1}).

Scheme I

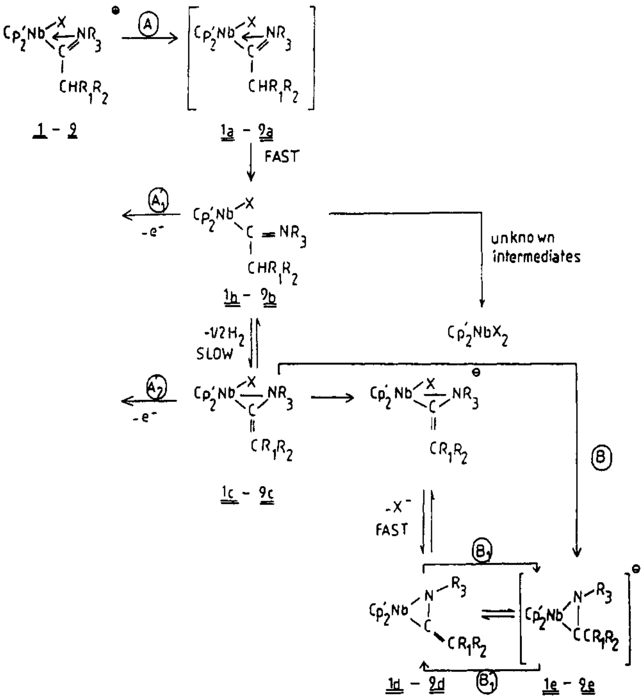

a mercury electrode consumes nearly 1 equiv of electrons, and red solutions were obtained from which after appropriate workup the ketenimine complexes $Nb(\eta^5\text{-}C_5H_4SiMe_3)_2X(\eta^2(C,N)\text{-}R^1R^2CCNR^3)$ were isolated. The cyclic voltammograms of the electrolyzed solutions were similar to those of the ketenimine complexes,[7] which are reduced at the potential of peak B. Trace amounts of the complexes $Nb(\eta^5C_5H_4SiMe_3)_2X_2$ (X = Cl, F) (identified by ESR spectroscopy) are also obtained in the electrolysis. For the bromo derivatives (**2**, **5**, **7**, and **9**) the same process consumes more than 1 electron (2 electrons for derivatives, **2**, **7**, and **9** and 1.5 electrons for derivative **5**) and a mixture of compounds was obtained; the ESR spectrum of the electrolyzed solutions shows two characteristic signals which correspond to both the $Nb(\eta^5C_5H_4SiMe_3)_2Br_2$ and the Nb(IV) ketenimine complex $Nb(\eta^5\text{-}C_5H_4SiMe_3)_2X(\eta^2(C,N)\text{-}R^1R^2CCNR^3)$.[7] These results can be partially rationalized according to Scheme I.

On the time scale of polarography, the reduction (peak A) of complexes **1–9** affords the very unstable intermediates **1a–9a** (19-electron species) which rapidly generate the niobium(IV) complexes **1b–9b**. The derivatives **1b**, **3b**, **8b**, and **9b** are unstable and they generate at room temperature the ketenimine complexes **1c**, **3c**, **8c**, and **9c** with evolution of H_2. This process is also observed for **2b** and **6b** by increasing the temperature to 50 °C. The derivatives **4b**, **5b**, and **7b** are relatively more stable, and this behavior could explain the absence in their polarograms of the reduction wave B.

On the time scale of cyclic voltammetry the intermediates **1b–9b** are oxidized at the potential of peak A'_1. The two-electron reduction (ECE process) of the Nb(V) derivatives **1c–9c**[7] (peak B) yields the anionic niobium complexes **1e–9e**, which are oxidized along peak B'_1 to give the paramagnetic ketenimine Nb(IV) complexes **1d–9d** (vide supra). Peak A'_2 corresponds to the oxidation of derivatives **1c–9c**. We have verified that the chemically prepared complexes **1c** and **2c** are oxidized at this potential.

On the time scale of electrolysis, the ketenimine complexes **1c**, **3c**, **4c**, **6c**, and **8c** are obtained after near one-electron reduction of the starting derivatives. The formation of $Nb(\eta^5\text{-}C_5H_4SiMe_3)_2X_2$ (X = Cl, F), in trace amounts, is difficult to explain, and we suggest that these compounds could be the result of a possible redistribution reaction of ligands from species such as $Nb(\eta^5\text{-}C_5H_4SiMe_3)_2RX$ (R = organic fragment from the ketenimine ligand). For the bromo derivatives (**2**, **5**, **7**, and **9**) the formation of the niobium(IV) complexes **2d**, **5d**, **7d**, and **9d** can be explained by an outer-sphere electron-transfer reaction between the electrogenerated anion $Nb(\eta^5\text{-}C_5H_4SiMe_3)_2Br_2^-$ and derivatives **2c**, **5c**, **7c**, and **9c**, respectively. This type of mechanism has been previously postulated for acetylenic niobium complexes.[17]

Chemical Reduction of η^2-Iminoacyl Complexes. We have investigated the reduction of the complexes **1–9** with 1 equiv of sodium amalgam. We have verified the electrochemical results; in fact, the iminoacyl complex reacts with 1 equiv of Na/Hg in THF at room temperature to give a red solution, from which the ketenimine complex was isolated. The H_2 resulting from this process was detected by a GC analysis of the gaseous phase, but in this work it was not quantified. As far as we know, this process has resulted in the first observation of a reduction reaction of an η^2-iminoacyl group to afford an η^2-ketenimine group.

X-ray Structures of $[Nb(\eta^5\text{-}C_5H_4SiMe_3)_2F(\eta^2\text{-}(C,N)\text{-}Ph_2HCCNPh)]^+BF_4^-$ (3) and $[Nb(\eta^5\text{-}C_5H_4SiMe_3)_2Cl(\eta^2(C,N)\text{-}EtPhHCCNPh)]^+BF_4^-$ (4). Although the complexes **3** and **4** crystallize in different monoclinic space groups, $P2_1/n$ and $C2/c$, respectively, which is due to the presence of different substituents on the iminoacyl ligand (Ph vs Et), their molecular structures exhibit the expected similar features. They consist of noninteracting cations and disordered fluoroborate anions. There is no carbon (cation)–fluorine (BF_4^-) contact shorter than 3.15 Å. The basic structural parameters of the cations and anions are closely similar. The ORTEP drawings of the cations **3** and **4** are given in Figures 4 and 5, respectively, and selected bond lengths and angles are presented in Table II. The cations have geometry typical of bent metallocenes with Nb–CP (CP is the gravity center of the cyclopentadienyl C_5 ligand) distances close to 2.11 Å and with CP1–Nb–CP2 angles equal to 130.7° (in **3**) and 130.1° (in **4**). The cyclopentadienyl rings are planar, with the Si atoms deviating from their best planes by 0.28 Å in **3** and 0.35 Å in **4** (supplementary material). The mutual orientation of the Cp′ rings in both complexes is intermediate between eclipsed and stagered, as indicated by the Si1–CP1–CP2/Si2–CP2–CP1 dihedral angles of 27 and 37° for **3** and **4**, respectively. A more eclipsed conformation

---

[17] Lucas, D.; Chollet, H.; Mugnier, Y.; Antiñolo, A.; Fajardo, M.; Otero, A. *J. Organomet. Chem.*, to be submitted for publication.

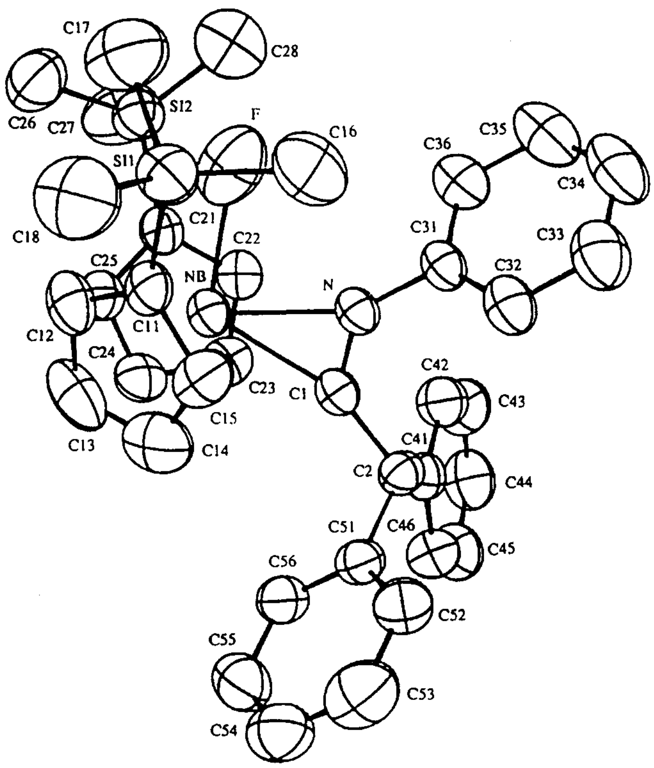

Figure 4. ORTEP drawing of the cation of 3, $[Nb(\eta^5\text{-}C_5H_4SiMe_3)_2F(\eta^2(C,N)\text{-}Ph_2HCCNPh)]^+$ (50% probability level). Only selected atoms are labeled for clarity.

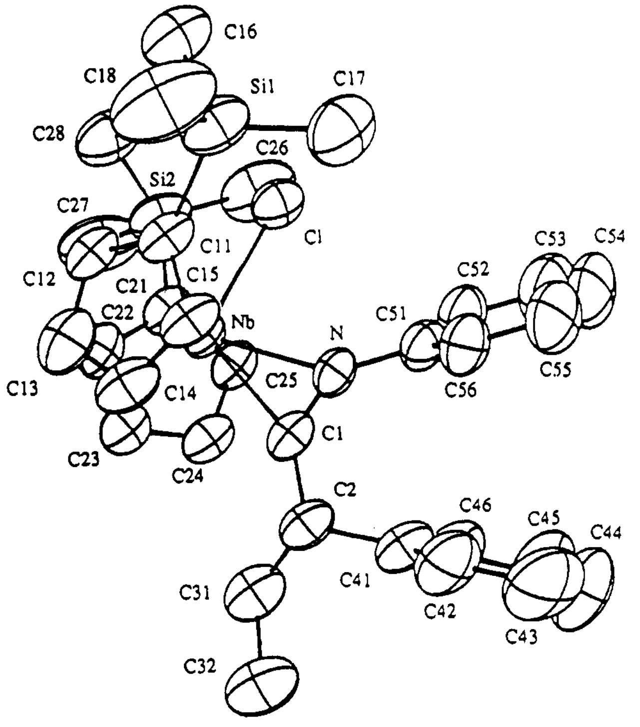

Figure 5. ORTEP drawing of the cation of 4, $[Nb(\eta^5\text{-}C_5H_4SiMe_3)_2Cl(\eta^2(C,N)\text{-}EtPhHCCNPh)]^+$ (50% probability level). Only selected atoms are labeled for clarity.

in 3 may be due to two factors: (i) the smaller size of the fluoride in 3 than that of the chloride in 4, suggesting the influence of the size of ligands in the bisecting plane on the conformation adopted by substituted or unsubstituted Cp ligands, and (ii) the better electron-withdrawing nature of fluoride than that of chloride. In bent molybdenocenes the latter electronic factor leads generally to the opening of the CP–Mo–CP angle in the presence of a better donor in the bisecting plane due to the enhanced repulsions between the rings.[18] Because the CP–Nb–CP angles in 3 and 4 are essentially the same, a removal of electron density from the rings by fluoride allows the Cp ligands to approach the energetically less favorable eclipsed conformation.

Table II. Selected Bond Distances (Å) and Angles (deg) for $[NbCp'_2X(\eta^2(C,N)\text{-}RPhHCCNPh)]^+$ Cations in 3 and 4

	X = F (3)	X = Cl (4)
Nb–X	2.199 (5)	2.468 (2)
Nb–N	2.157 (4)	2.148 (5)
Nb–C1	2.180 (5)	2.170 (5)
Nb–CP1	2.110	2.116
Nb–CP2	2.105	2.110
N–C1	1.253 (7)	1.23 (1)
C1–C2	1.517 (8)	1.51 (1)
N–Ph	1.417 (7)[a]	1.43 (1)[b]
CP1–Nb–CP2	130.7	130.1
X–Nb–N	78.6 (2)	80.4 (2)
X–Nb–C1	112.1 (2)	113.5 (3)
N–Nb–C1	33.6 (2)	33.2 (4)
Nb–C1–N	72.3 (3)	72.4 (3)
Nb–C1–C2	158.9 (4)	151.5 (6)
N–C1–C2	128.9 (5)	135.7 (6)
Nb–N–C1	74.2 (3)	74.4 (4)
Nb–N–Ph	151.7 (4)[a]	147.2 (5)[b]
C1–N–Ph	133.9 (5)[a]	137.3 (6)[b]

[a] Ph = C31. [b] Ph = C51.

The Nb–Cl bond length in 4 (2.468 (2) Å) is close to the values of 2.483 (2) and 2.470 (5) Å observed in $Cp_2Nb^V(O)_2Cl$[19] and $Cp_2Nb^{IV}Cl_2$[20] complexes, respectively. It is longer than the corresponding distances found in $Cp_2Nb^V(O)Cl$ (2.439 (2) Å)[21] and in the $[(Cp_2Nb^VCl)_2O]^{2+}$ cation (2.370 (4) Å),[20] where only two coordinated sites of the Nb atom in the bisecting plane are occupied. The Nb–F distance in -3 (2.199 (5) Å) is shorter, as expected, and to our knowledge complex 3 is the first niobocene derivative with Nb–F bonding which has been structurally characterized.

The Nb, X, N, and C1 atoms (X = F in 3; X = Cl in 4) are essentially coplanar, with deviations from the best least-squares plane not exceeding 0.03 Å. A set of these atoms, with two supplementary carbon atoms bonded to N and to C1, remains roughly planar with the largest deviation equal to 0.07 Å.

The structural parameters in the η^2-iminoacyl ligands in 3 and 4 are closely similar, and the geometry of the Nb–$\eta^2(C,N)$-CC fragment is reminiscent of that observed in η^2-iminoacyl complexes of vanadium, titanium, zirconium, tantalum, and molybdenum.[2f,i,4a,b5,22] The Nb–N bond lengths of 2.157 (4) Å in 3 and 2.148 (5) Å in 4 are longer than the V–N bond length in $[VCp_2(\eta^2\text{-}PhCNMe)]^+$ (2.054 (4) Å),[5] which is evidently due to a difference in covalent radii of V and Nb, but they are essentially the same as the corresponding M–N distances found in $[Ta(OAr\text{-}2,6\text{-}Me_2)_2(\eta^2\text{-}MeCNAr\text{-}2,6\text{-}Me_2)_2Me]$ (2.151 (5) and 2.165 (5) Å)[4a] and in $[MoCp'(CO)_2(\eta^2\text{-}MeCNPh)]$ (2.143 (4) Å).[22] The Nb–C1 bond lengths of 2.180 (5) and 2.170 (5) Å are slightly shorter than in the tantalum complex (2.187 (7) and 2.200 (6) Å)[4a] but significantly longer than

---

(18) Kubicki, M. M.; Kergoat, R.; Guerchais, J. E.; Bkouche-Waksman, I.; Bois, C.; L'Haridon, P. *J. Organomet. Chem.* **1981**, *219*, 329.

(19) Bkouche-Waksman, I.; Bois, C.; Sala-Pala, J.; Guerchais, J. E. *J. Organomet. Chem.* **1980**, *195*, 307.

(20) Prout, K.; Cameron, T. S.; Forder, R. A.; Critchley, S. R.; Denton, B.; Ries, G. V. *Acta Crystallogr.* **1974**, *B30*, 2290.

(21) Rheingold, A. L.; Strong, J. B. *Acta Crystallogr.* **1991**, *C47*, 1963.

(22) Adams, R. D.; Chodosh, D. F. *Inorg. Chem.* **1978**, *17*, 41.

the value of 2.106 (5) Å observed in the molybdenum complex.[22] They are slightly longer than the corresponding values found in the Nb-acyl complex $[NbCp'_2Cl(\eta^2\text{-}EtPhHCCO)]^+$ (2.121 (5) Å)[8a] and in $NbCp'_2Br(\eta^2\text{-}Ph_2C{=}C{=}O)$ (2.145 (3) and 2.132 (3) Å).[8b] The N–C1 bond lengths of 1.253 (7) Å in **3** and 1.23 (1) Å in **4** fall in the range of 1.233 (6)–1.286 (8) Å observed in all known η^2-iminoacyl structures. Such a narrow range of η^2-CN distances indicates that the nature of bonding of this formally two-center–three-electron donor ligand with different metals is similar. The observed range is shorter than the 1.29–1.31 Å generally accepted for an uncoordinated double bond[22,23] but also significantly longer than the 1.14–1.16 Å found for C–N triple bonds in organonitriles.[23] Thus, the C–N bond is strengthened upon η^2 coordination of iminoacyl, indicating electron delocalization over the NbNC propene-like fragment with clear implication of the nitrogen lone pair in the bonding. The iminoacyl ligand resembles a coordinated alkyne. It is well-known that upon coordination the substituents of the linear acetylene fold back away from the coordination site. The fold angle is known to range from 138 to 172°[23] but generally lies in the range 140–150°. This is similar to the values of our fold or "bent-back" angles N–C1–C2, equal to 128.9 (5)° in **3** and 135.7 (6)° in **4**, and C1–N–Ph, equal to 133.9 (5)° in **3** and 137.3 (6)° in **4**.

The phenyl groups (C31–C36 in **3**, C51–C56 in **4**) are tilted with respect to the NbXNC1 planes by 49 and 61° in **3** and **4**, respectively, suggesting that there is little or no conjugation between η^2-CN and Ph fragments. Other geometrical parameters in the cation are normal.

Experimental Section

All manipulations were performed by using standard Schlenk techniques under an atmosphere of dry, oxygen-free nitrogen or argon. Solvents were purified by distillation from appropriate drying/deoxygenating agents prior to use.[24]

Elemental analyses were performed with a Perkin-Elmer 240B microanalyzer. NMR spectra were recorded on a Varian Unity 300-MHz spectrometer. ^1H and ^{13}C chemical shifts are reported versus Me_4Si and were determined by reference to the residual ^1H and ^{13}C solvent peaks. IR spectra were recorded as Nujol mulls between CsI plates in the region 4000–200 cm^{-1} with a Perkin-Elmer PE883 IR spectrometer. For voltammetry experiments the working electrode was a platinum disk (diameter 1.2 mm) and for the controlled potential electrolyses a platinum grid. In all cases, the reference electrode was a saturated calomel electrode (SCE) separated from the solution by a sintered-glass disk. The auxiliary electrode was a platinum wire. For thin-layer cyclic voltammetry (TLCV) the platinum-disk electrode was lowered until it came in contact with the floor of the electrolytic cell so that only a thin layer of solution existed between them. For the rotating-disk experiments, a three-electrode Tacussel Tipol polarograph was used. The cyclic voltammetry experiments were conducted with a Tacussel UAP4 unit connected to a Tektronix 5115 oscilloscope or a Sefram TGM 164 X-Y recorder. The macroelectrolyses were carried out with an Amel 552 potentiostat equipped with a Tacussel IG5 integrator.

$Nb(\eta^2\text{-}C_5H_4SiMe_3)_2X(\eta^2(C,N)\text{-}R^1R^2CCNR^3)$ and $Nb(\eta^5\text{-}C_5H_4SiMe_3)_2(\eta^2(C,N)\text{-}Ph_2CCNPh)$ were prepared according to published methods.[7]

$[Nb(\eta^5\text{-}C_5H_4SiMe_3)_2X(\eta^2(C,N)\text{-}R^1R^2HCCNR^3)]^+BF_4^-$ (X = Cl, $R^1 = R^2 = R^3 = C_6H_5$, 1; X = Br, $R^1 = R^2 = R^3 = C_6H_5$, 2; X = F, $R^1 = R^2 = R^3 = C_6H_5$, 3; X = Cl, $R^1 = R^3 = C_6H_5$, $R^2 = C_2H_5$, 4; X = Br, $R^1 = R^3 = C_6H_5$, $R^2 = C_2H_5$, 5; X = Cl, $R^1 = R^3 = C_6H_5$, $R^2 = CH_3$, 6; X = Br, $R^1 = R^2 = C_6H_5$, $R^2 = CH_3$, 7; X = Cl, $R^1 = R^2 = C_6H_5$, R^3 = *p*-Br-C_6H_4, 8; X = Br, $R^1 = R^2 = C_6H_5$, R^3 = *p*-Br-C_6H_4, 9). To a red solution of $Nb(\eta^5\text{-}C_5H_4SiMe_3)_2Cl(\eta^2(C,N)\text{-}Ph_2CCNPh)$ (400 mg, 0.59 mmol) in 30 mL of diethyl ether was added 0.59 mmol of $HBF_4{\cdot}OEt_2$. The solution was stirred, and immediately a white precipitate was formed with bleaching of the red color. The solid was isolated by filtration, and then it was recrystallized from a mixture (1:1) of dichloromethane–hexane. The colorless air-stable crystals were identified as the complex **1**. Derivatives **2–9** were obtained by identical procedures.

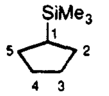

1: IR(Nujol) ν(C=N) 1717 cm^{-1}, ^1H NMR ($CDCl_3$) δ –0.04 (s, 18H, Si*Me*$_3$), 5.83 (4H) and 6.18 (4H), (each a complex signal, C_5H_4), 6.56 (s, 1 H, C*H*Ph$_2$), 7.00–7.20 (m, 15H, *Ph*); $^{13}C\{^1H\}$ NMR ($CDCl_3$) δ –0.5 (Si*Me*$_3$), 58.4 (*C*HPh$_2$), 114.4 (C1), 108.7, 109.9, 122.5, and 124.4 (C2, C3, C4, C5; exact assignment not possible), 128.4, 128.6, 128.8, 129.3, 129.4, and 132.2 (C of phenyl groups), 135.7, 136.2 (C(ipso) of phenyl groups), 213.6 (*C*=N). Anal. Found (calcd) for $C_{36}H_{42}BClF_4NNbSi_2$): C, 55.99 (56.89); H, 5.34 (5.57); N, 1.72 (1.84). Yield: 90%.

2: IR (Nujol) ν(C=N) 1716 cm^{-1}; ^1H NMR ($CDCl_3$) δ 0.16 (s, 18H, Si*Me*$_3$), 6.18 (2H), 6.34 (2H), and 6.42 (2 H) (each a complex signal, C_5H_4), 6.78 (s, 1H, C*H*Ph$_2$), 7.20–7.40 (m, 15 H, Ph); $^{13}C\{^1H\}$ NMR ($CDCl_3$) δ 0.04 (Si*Me*$_3$), 57.9 (*C*HPh$_2$), 116.2 (C1), 107.6, 110.3, 124.3, and 125.2 (C2, C3, C4, C5; exact assignment not possible), 128.7, 128.8, 128.9, 129.0, 129.4, and 129.6 (C of phenyl groups), 135.8 and 135.9 (C(ipso) of phenyl groups), 209.7 (*C*=N). Anal. Found (calcd) for $C_{36}H_{42}BBrF_4NNbSi_2$: C, 53.70 (53.74); H, 5.56 (5.26); N, 1.64 (1.74). Yield: 90%.

3 (N-inside isomer): IR (Nujol) ν(C=N) 1661 cm^{-1}; ^1H NMR ($CDCl_3$) δ 0.09 (s, 18H, Si*Me*$_3$), 5.92 (2H), 5.98 (2H), 6.48 (2H), and 6.58 (2H) (each a complex signal, C_5H_4), 6.64 (s, 1H, C*H*Ph$_2$), 7.10–7.30 (m, 15H, Ph); $^{13}C\{^1H\}$ NMR ($CDCl_3$) δ –1.4 (Si*Me*$_3$), 58.8 (*C*HPh$_2$), 109.1, 111.4, 112.2, 119.9, and 124.9 (C1, C2, C3, C4, C5; exact assignment not possible), 128.6, 129.2, 129.3, 129.4, and 129.7 (C of phenyl groups), 136.9 and 138.2 (C(ipso) of phenyl groups), 221.4 (*C*=N). Anal. Found (calcd) for $C_{36}H_{42}BF_5NNbSi_2$: C, 58.89 (58.14); H, 5.63 (5.70); N, 1.89 (1.88). Yield: 90%.

4: IR (Nujol) ν(C=N) 1707 cm^{-1}; ^1H NMR ($CDCl_3$) δ 0.18 (s, 9 H, Si*Me*$_3$) and 0.21 (s, 9H, Si*Me*$_3$) (two different signals for the $C_5H_4SiMe_3$ diastereotopic species), 1.01 (t, 3H, C*H*$_3$, *J* = 7.0 Hz), 2.38 (m, 2H, $CHCH_AH_BCH_3$), 5.05 (dd, 1H, $CHCH_ACH_B$, *J* = 4.4 Hz, *J* = 10.9 Hz), 5.92 (1H), 5.97 (1H), 6.04 (1H), 6.16 (1H), 6.43 (3H), and 6.72 (1H) (each a complex signal, C_5H_4), 7.15–7.60 (m, 10H, Ph); $^{13}C\{^1H\}$ NMR ($CDCl_3$) δ –0.3 (Si*Me*$_3$), 11.9 ($CHCH_2CH_3$), 27.1 ($CHCH_2CH_3$), 55.3 (PhEt*C*H), 108.3, 108.5, 109.8, 111.4, 115.1, 115.7, 122.5, 123.3, 124.0, and 124.0 (C1, C2, C3, C4, C5 for the two $C_5H_4SiMe_3$ diastereotopic species; exact assignment not possible), 128.7, 128.8, 128.9, 129.1, 129.4, and 129.7 (C of phenyl groups), 135.9 and 136.1 (C(ipso) of phenyl groups), 215.7 (C=N). Anal. Found (calcd) for $C_{36}H_{42}BClF_4NNbSi_2$: C, 53.86 (53.98); H, 6.33 (5.94); N, 1.97 (1.94). Yield: 91%.

5: IR (Nujol) ν(C=N) 1689 (cm^{-1}; ^1H NMR ($CDCl_3$) δ 0.19 (s, 9H, Si*Me*$_3$) and 0.21 (s, 9H, Si*Me*$_3$) (two different signals for the $C_5H_4SiMe_3$ diastereotopic species), 0.97 (t, 3H, C*H*$_3$, *J* = 7.1 Hz), 2.16 (m, 1H, $CHCH_AH_BCH_3$), 2.32 (m, 1H, $CHCH_AH_BCH_3$), 5.06 (dd, 1H, $CHCH_AH_BCH_3$, *J* = 4.8 Hz, *J* = 10.1 Hz), 5.93 (1H), 6.01 (1H), 6.05 (2H), 6.38 (1H), 6.49 (2H), and 6.63 (1H) (each a complex signal, C_5H_4), 7.15–7.40 (m, 10H, Ph); $^{13}C\{^1H\}$ NMR ($CDCl_3$) δ 0.1 (Si*Me*$_3$), 12.0 ($CHCH_2CH_3$), 27.3 ($CHCH_2CH_3$), 54.9 (PhEt*C*H), 106.9, 107.7, 110.7, 110.9, 116.9, 117.5, 123.9, 124.2, and 124.8 (C1, C2, C3, C4, C5 for the two $C_5H_4SiMe_3$ diastereotopic species; exact assignment not possible), 128.9, 129.1, 129.3, and 129.9 (C of phenyl groups), 135.6 and 136.3 (C(ipso) of phenyl groups), 211.9 (*C*=N). Anal. Found (calcd)

---

(23) Allen, F. H.; Kennard, O.; Watson, D. G.; Brammer, L.; Orpen, A. G.; Taylor, R. *J. Chem. Soc., Perkin Trans. 2* 1987, S1.

(24) Perrin, D. D.; Armarego, W. L. F.; Perrin, D. R. *Purification of Laboratory Chemicals*; Pergamon: New York, 1980.

Table III. Crystallographic Data for (Iminoacyl)niobium Complexes

	3	4
mol formula	$C_{36}H_{42}NbNSi_2BF_5$	$C_{32}H_{42}NbClNSi_2BF_4$
fw	743.62	712.03
cryst syst	monoclinic	monoclinic
space group	$P2_1/n$ (No. 14)	$C2/c$ (No. 15)
cell dimens		
a, Å	11.004 (4)	23.962 (8)
b, Å	17.702 (5)	21.408 (5)
c, Å	18.679 (4)	16.456 (3)
β, deg	91.60 (2)	123.30 (2)
V, Å^3	3637.3	7055.5
Z	4	8
ρ_{calcd}, g cm^{-3}	1.358	1.368
linear abs, μ, cm^{-1}	4.301	4.76
$F(000)$	1536	2944
λ(Mo Kα radiation), Å	0.710 73	
scan type	ω–2θ	
scan speed, deg min^{-1}	1.0–8.3	
scan width, deg	$\Delta\omega = 0.9 + 0.347 \tan\theta$	
octants collcd	$\pm h,k,l$	$h,k,\pm l$
θ range, deg	2–25	2–23
no. of rflns measd	6832	5856
temp, K	296 (1)	
decay, %	−1.4, cor	−1.4, cor
transmissn coeff (Ψ scan)	93.711–99.865	not cor
cutoff for obsd data	$I > 3\sigma(I)$	$I > 3\sigma(I)$
no. of unique data (NO)	4056	3197
no. of variables (NV)	394	244
$R(F)$	0.051	0.046
$R_w(F)$	0.058	0.048
g in $w = 1/[\sigma^2(F) + gF^2]$	0.0011	0.0003
GOF	1.572	1.871

Table IV. Positional Parameters and Their Estimated Standard Deviations for $[Nb(\eta^5\text{-}C_5H_4SiMe_3)_2F(\eta^2(C,N)\text{-}Ph_2HCCNPh)]^+BF_4^-$ (3)[a]

atom	x	y	z	B, Å^2
Nb	0.30892 (4)	0.31079 (3)	0.47477 (3)	3.38 (1)
F	0.3162 (4)	0.2132 (3)	0.5476 (3)	8.5 (1)
N	0.4276 (4)	0.2353 (3)	0.4189 (2)	3.3 (1)
C1	0.4245 (5)	0.2952 (3)	0.3831 (3)	3.3 (1)
C2	0.4886 (5)	0.3137 (3)	0.3144 (3)	3.5 (1)
C31	0.4821 (5)	0.1637 (3)	0.4093 (3)	3.5 (1)
C32	0.4679 (5)	0.1261 (3)	0.3446 (4)	4.5 (2)
C33	0.5232 (6)	0.0559 (4)	0.3376 (5)	6.0 (2)
C34	0.5887 (7)	0.0240 (4)	0.3941 (5)	6.7 (2)
C35	0.5994 (7)	0.0613 (4)	0.4584 (5)	6.7 (2)
C36	0.5453 (6)	0.1317 (4)	0.4670 (4)	5.2 (2)
C41	0.6092 (5)	0.3551 (3)	0.3290 (3)	3.8 (1)
C42	0.6870 (6)	0.3329 (4)	0.3855 (4)	5.3 (2)
C43	0.7979 (6)	0.3674 (5)	0.3971 (4)	6.3 (2)
C44	0.8353 (6)	0.4237 (5)	0.3527 (5)	6.5 (2)
C45	0.7629 (6)	0.4451 (5)	0.2954 (4)	6.2 (2)
C46	0.6482 (6)	0.4109 (4)	0.2830 (4)	5.0 (2)
C51	0.4005 (5)	0.3528 (3)	0.2628 (3)	3.8 (1)
C52	0.3537 (6)	0.3110 (4)	0.2047 (3)	4.8 (2)
C53	0.2706 (7)	0.3451 (6)	0.1586 (4)	6.9 (2)
C54	0.2314 (7)	0.4168 (5)	0.1686 (4)	6.3 (2)
C55	0.2752 (6)	0.4580 (4)	0.2269 (4)	5.9 (2)
C56	0.3615 (5)	0.4264 (4)	0.2741 (3)	4.5 (2)
Si1	0.0713 (2)	0.1455 (1)	0.4828 (1)	4.92 (5)
C11	0.1155 (4)	0.2431 (3)	0.4540 (3)	3.8 (1)
C12	0.0935 (5)	0.3111 (4)	0.4910 (4)	4.9 (2)
C13	0.1197 (6)	0.3719 (4)	0.4470 (6)	6.3 (2)
C14	0.1605 (6)	0.3419 (5)	0.3815 (5)	6.6 (2)
C15	0.1580 (5)	0.2646 (5)	0.3871 (3)	4.9 (2)
C16	0.1628 (8)	0.0768 (4)	0.4332 (5)	7.5 (2)
C17	0.0877 (9)	0.1309 (6)	0.5803 (5)	8.8 (3)
C18	−0.0919 (7)	0.1381 (5)	0.4562 (5)	8.1 (3)
Si2	0.3860 (2)	0.3100 (1)	0.6820 (1)	5.32 (5)
C21	0.3902 (5)	0.3563 (3)	0.5921 (3)	4.1 (1)
C22	0.4867 (5)	0.3553 (4)	0.5421 (3)	4.2 (2)
C23	0.4619 (6)	0.4079 (4)	0.4879 (4)	4.9 (2)
C24	0.3484 (6)	0.4417 (4)	0.4997 (4)	4.8 (2)
C25	0.3050 (6)	0.4088 (4)	0.5638 (3)	4.5 (2)
C26	0.2271 (7)	0.3051 (5)	0.7121 (4)	7.3 (2)
C27	0.475 (1)	0.3753 (6)	0.7407 (5)	10.2 (3)
C28	0.457 (1)	0.2156 (6)	0.6816 (6)	11.4 (4)
B	0.353 (1)	0.1028 (8)	0.1169 (8)	8*
F1	0.3243 (7)	0.1671 (4)	0.0810 (4)	12*
F2	0.248 (1)	0.0641 (7)	0.1178 (6)	11*
F21	0.318 (2)	0.035 (1)	0.108 (1)	12*
F3	0.417 (1)	0.0600 (7)	0.0709 (6)	12*
F31	0.465 (1)	0.1147 (9)	0.1387 (9)	13*
F4	0.399 (2)	0.113 (1)	0.182 (1)	14*
F41	0.296 (1)	0.1224 (7)	0.1902 (7)	11*
CP1	0.1294	0.3065	0.4321	
CP2	0.3984	0.3940	0.5371	

[a] CP stands for the gravity centers of the cyclopentadienyl rings. Starred values denote atoms refined isotropically. Anisotropically refined atoms are given in the form of the isotropic equivalent displacement parameter, defined as $^4/_3[a^2B_{11} + b^2B_{22} + c^2B_{33} + ab(\cos\gamma)B_{12} + ac(\cos\beta)B_{13} + bc(\cos\alpha)B_{23}]$.

for $C_{32}H_{42}BBrF_4NNbSi_2$: C, 50.78 (50.81); H, 5.86 (5.59); N, 1.71 (1.85). Yield: 90%.

6: IR (Nujol) ν(C═N) 1708 cm^{-1}; ^{1}H NMR ($CDCl_3$) δ 0.12 (s, 9H, Si*Me*$_3$) and 0.21 (s, 9H, Si*Me*$_3$) (two different signals for the $C_5H_4SiMe_3$ diastereotopic species), 1.96 (d, 3H, C*H*$_3$), 5.34 (q, 1H, C*H*CH$_3$), 5.79 (1H), 5.94 (1H), 6.12 (1H), 6.28 (1H), 6.38 (1H), 6.47 (2H), 6.68 (1H) (each a complex signal, C$_5$*H*$_4$), 7.12–7.54 (m, 10H, Ph); $^{13}C\{^1H\}$ NMR ($CDCl_3$) δ −0.3 (Si*Me*$_3$), −0.2 (Si*Me*$_3$) (two different signals for the $C_5H_4SiMe_3$ diastereotopic species), 19.3 (CH*C*H$_3$Ph), 47.3 (*C*HCH$_3$Ph), 107.1, 108.9, 109.2, 112.2, 115.7, 116.4, 123.3, 123.4, 124.1, and 124.1 (C1, C2, C3, C4, C5 for the two $C_5H_4SiMe_3$ diastereotopic species; exact assignment not possible), 128.3, 128.7, 128.9, 129.4, and 129.59 (C of phenyl groups), 136.0 and 137.7 (C(ipso) of phenyl groups), 216.2 (*C*═N). Anal. Found (calcd) for $C_{31}H_{40}BClF_4NNbSi_2$: C, 53.40 (53.34); H, 5.74 (5.77); N, 1.95 (2.01). Yield: 90%.

7: IR (Nujol) ν(C═N) 1704 cm^{-1}; ^{1}H NMR ($CDCl_3$) δ 0.16 (s, 9H, Si*Me*$_3$) and 0.24 (s, 9H, Si*Me*$_3$) (two different signals for the $C_5H_4SiMe_3$ diastereotopic species), 0.95 (d, 3H, C*H*$_3$), 5.35 (q, 1H, C*H*CH$_3$), 5.72 (1H), 6.14 (1H), 6.20 (1H), 6.24 (1H), 6.28 (1H), 6.48 (1H), 6.55 (1H), 6.58 (1H) (each a complex signal, C$_5$*H*$_4$), 7.10–7.54 (m, 10H, Ph); $^{13}C\{^1H\}$ NMR ($CDCl_3$) δ 0.07 (Si*Me*$_3$), 0.12 (Si*Me*$_3$) (two different signals for the C_5H_4SiMe diastereotopic species), 19.3 (CH*C*H$_3$Ph), 46.8 (*C*HCH$_3$Ph), 106.3, 107.8, 109.3, 112.9, 117.2, 118.4, 124.1, 124.3, and 125.2 (C1, C2, C3, C4, C5 for the two $C_5H_4SiMe_3$ diastereotopic species; exact assignment not possible), 128.4, 128.8, 129.0, 129.3, and 129.7 (C of phenyl groups), 136.2 and 137.5 (C(ipso) of phenyl groups), 215.4 (*C*═N). Anal. Found (calcd) for $C_{31}H_{40}BBrF_4NNbSi_2$: C, 49.63 (50.15); H, 5.55 (5.43); N, 1.68 (1.89).

8: IR (Nujol) ν(C═N) 1677 cm^{-1}; ^{1}H NMR ($CDCl_3$) δ 0.16 (s, 18H, Si*Me*$_3$), 6.02 (4H), 6.34 (2H), 6.38 (2H) (each a complex signal, C$_5$*H*$_4$), 6.81 (s, 1H, C*H*Ph$_2$), 6.60–7.50 (m, 14H, Ph and *p*-Br-C_6H_4); $^{13}C\{^1H\}$ NMR ($CDCl_3$) δ −0.3 (Si*Me*$_3$), 58.7 (*C*HPh$_2$), 109.0, 110.3, 113.7, 123.6, and 126.0 (C1, C2, C3, C4, C5; exact assignment not possible), 128.8, 129.4, 129.6, 130.8, and 132.1 (C of phenyl groups), 134.8 and 136.1 (C(ipso) of phenyl groups), 215.5 (C═). Anal. Found (calcd) for $C_{36}H_{41}BBrClF_4NNbSi_2$: C, 51.08 (51.54); H, 4.91 (4.92); N, 1.64 (1.67). Yield: 95%.

9: IR (Nujol) ν(C═N) 1679 cm^{-1}; ^{1}H NMR ($CDCl_3$) δ 0.19 (s, 18H, Si*Me*$_3$), 5.96 (2H), 6.22 (2H), 6.33 (2H), and 6.40 (2H) (each a complex signal, C$_5$*H*$_4$), 6.80 (s, 1H, C*H*Ph$_2$), 7.25–7.44 (m, 14H, Ph and *p*-Br-C_6H_4); $^{13}C\{^1H\}$ NMR ($CDCl_3$) δ 0.0 (Si*Me*$_3$), 58.3 (*C*HPh$_2$), 107.9, 110.3, 115.5, 122.8, 126.0 (C1, C2, C3, C4, C5; exact assignment not possible), 128.9, 129.4, 129.6 and 131.9 (C of phenyl groups), 135.9 (C(ipso) of phenyl groups), 211.4 (*C*═N). Anal. Found (calcd) for $C_{36}H_{41}BBr_2F_4NNbSi_2$: C, 48.78 (48.94); H, 5.01 (4.68); N, 1.58 (1.58). Yield: 95%.

Preparation of the Mixture of N-Outside and N-Inside Isomers of $[Nb(\eta^5\text{-}C_5H_4SiMe_3)_2F(\eta^2(C,N)\text{-}Ph_2HCCNPh)]^+BF_4^-$ from $Nb(\eta^5\text{-}C_5H_4SiMe_3)_2(\eta^2(C,N)\text{-}Ph_2CCNPh)$. To a brown solution of $Nb(\eta^5\text{-}C_5H_4SiMe_3)_2(\eta^2(C,N)\text{-}Ph_2CCNPh)$ (360 mg, 0.50 mmol) in 50 mL of diethyl ether was added dropwise a solution of $HBF_4\cdot OEt_2$ (1.00 mmol) at −20 °C. The mixture was allowed to react with stirring over 24 h. Liberation of H_2 was

Table V. Positional Parameters and Their Estimated Standard Deviations for $[Nb(\eta^5\text{-}C_5H_4SiMe_3)_2Cl(\eta^2(C,N)\text{-}EtPhHCCNPh]^+BF_4^-$ (4)[a]

atom	*x*	*y*	*z*	*B*, Å^2
Nb	0.18194 (3)	0.16000 (3)	0.21221 (4)	3.43 (2)
Cl	0.21161 (9)	0.16917 (8)	0.0909 (1)	5.17 (6)
N	0.2855 (3)	0.1340 (2)	0.3010 (4)	4.0 (2)
C1	0.2653 (3)	0.1335 (3)	0.3557 (5)	4.0 (2)
C2	0.2967 (4)	0.1245 (3)	0.4633 (5)	5.0 (2)
C31	0.2531 (4)	0.0862 (4)	0.4846 (5)	6.5 (3)
C32	0.2805 (5)	0.0828 (4)	0.5931 (5)	8.4 (4)
C41	0.3677 (4)	0.1015 (4)	0.5153 (5)	5.4 (3)
C42	0.4193 (5)	0.1387 (5)	0.5842 (6)	7.8 (3)
C43	0.4863 (7)	0.1170 (8)	0.6326 (9)	11.3 (6)
C44	0.4960 (8)	0.059 (1)	0.611 (1)	12.7 (7)
C45	0.4488 (7)	0.0224 (7)	0.546 (1)	12.5 (6)
C46	0.3831 (5)	0.0438 (4)	0.4975 (6)	7.9 (4)
C51	0.3483 (4)	0.1302 (4)	0.3099 (5)	4.8 (2)
C52	0.3546 (4)	0.0878 (4)	0.2521 (6)	6.5 (3)
C53	0.4164 (5)	0.0840 (5)	0.2617 (7)	9.2 (4)
C54	0.4668 (5)	0.1232 (6)	0.3248 (8)	9.3 (4)
C55	0.4595 (4)	0.1661 (5)	0.3792 (7)	8.5 (4)
C56	0.3988 (4)	0.1702 (4)	0.3707 (5)	6.2 (3)
Si1	0.2280 (1)	0.3235 (1)	0.1419 (2)	6.45 (8)
C11	0.1906 (4)	0.2750 (3)	0.1969 (5)	4.5 (2)
C12	0.1233 (4)	0.2572 (3)	0.1559 (5)	4.8 (2)
C13	0.1148 (4)	0.2359 (3)	0.2287 (6)	6.4 (3)
C14	0.1773 (4)	0.2358 (3)	0.3155 (6)	5.7 (3)
C15	0.2241 (4)	0.2609 (3)	0.2964 (5)	4.8 (2)
C16	0.1721 (4)	0.3243 (4)	0.0073 (6)	8.0 (3)
C17	0.3149 (4)	0.2999 (4)	0.1880 (6)	8.1 (3)
C18	0.2312 (6)	0.4033 (4)	0.1879 (8)	12.1 (5)
Si2	0.0662 (1)	0.0907 (1)	−0.0540 (2)	6.54 (8)
C21	0.1018 (3)	0.0895 (3)	0.0812 (5)	4.6 (2)
C22	0.0703 (3)	0.1150 (3)	0.1250 (5)	5.0 (3)
C23	0.1039 (4)	0.0961 (3)	0.2220 (5)	4.9 (3)
C24	0.1559 (4)	0.0558 (3)	0.2392 (5)	4.9 (2)
C25	0.1562 (3)	0.0535 (3)	0.1542 (5)	4.4 (2)
C26	0.0433 (4)	0.1705 (4)	−0.1019 (6)	7.8 (3)
C27	−0.0119 (5)	0.0442 (5)	−0.1092 (6)	11.2 (5)
C28	0.1244 (5)	0.0509 (4)	−0.0791 (6)	9.7 (4)
B	0.0979 (6)	0.1775 (5)	0.4641 (8)	6.7 (2)*
F1	0.1552 (3)	0.2126 (2)	0.4893 (4)	8.0 (1)*
F2	0.0762 (6)	0.1911 (5)	0.5187 (8)	7.8 (3)*
F21	0.0508 (5)	0.2152 (5)	0.4622 (8)	7.4 (2)*
F3	0.1037 (6)	0.1150 (6)	0.460 (1)	9.8 (3)*
F31	0.1215 (7)	0.1357 (7)	0.542 (1)	12.0 (4)*
F4	0.0534 (6)	0.1933 (6)	0.3627 (9)	9.7 (3)*
F41	0.0778 (5)	0.1450 (5)	0.3867 (8)	7.9 (2)*
CP1	0.1660	0.2530	0.2387	
CP2	0.1176	0.0820	0.1643	

[a] See footnote *a* in Table IV.

observed, which was detected by a GC analysis of the gaseous phase, and the solution became red to give finally a light brown precipitate. The solid was crystallized by dissolving it in dichloromethane and placing a layer of hexane above it in a Schlenk tube. In this general procedure we have always isolated the mixture of both conformers enriched in the N-inside conformer, which was obtained as a pure sample by means of two recrystallizations. The N-outside conformer has also been isolated in small amounts by recrystallization (mixture of dichloromethane and hexane) of samples previously enriched in this conformer. 3 (N-outside isomer): IR (Nujol) ν(C=N) 1663 cm^{-1}; ^{1}H NMR (CDCl$_3$) δ 0.18 (s, 18H, Si*Me*$_3$), 4.45 (2H), 5.24 (2H), 5.94 (2H), and 6.04 (2H) (each a complex signal, C$_5$H$_4$), 6.30 (s, 1H, C*H*Ph$_2$), 7.30–7.45 (m, 15H, Ph); ^{13}C{^{1}H} NMR (CDCl$_3$) δ −0.08 (Si*Me*$_3$), 57.4 (*C*HPh$_2$), 101.3, 103.5, 104.6, 114.8, and 124.0 (C1, C2, C4, C4, C5; exact assigment not possible), 128.3, 128.9, 129.2, 129.4, and 129.6 (C of phenyl groups), 135.5, 137.3 (C(ipso) of phenyl groups), 217.2 (C=N). Anal. Found (calcd) for $C_{36}H_{42}BF_5NNbSi_2$: C, 58.65 (58.14); H, 5.67 (5.70); N, 1.90 (1.88).

Reduction of $[Nb(\eta^5\text{-}C_5H_4SiMe_3)_2X(\eta^2(C,N)\text{-}R^1R^2\text{-}HCCNR^3)]^+BF_4^-$ (1–9) with Na/Hg. A mixture of $[Nb(\eta^5\text{-}C_5H_4SiMe_3)_2Cl(\eta^2(C,N)\text{-}Ph_2HCCNPh]^+BF_4^-$ (400 mg, 0.54 mmol) and Na/Hg (0.54 mmol) in 30 mL of THF was vigorously stirred for 2 h at room temperature. The solution became increasingly red, and then the solvent was removed in vacuo and the resulting impure red solid was dissolved in hexane. The red filtrate was concentrated and cooled to give red crystals of $[Nb(\eta^5\text{-}C_5H_4SiMe_3)_2Cl(\eta^2(C,N)\text{-}Ph_2C{=}C{=}NPh]$. H$_2$ was detected by GC analysis of the gaseous phase. Complexes 2–9 react with Na/Hg in a similar way.

Crystal Structure Analyses. Crystals of 3 (yellow; 0.4 × 0.3 × 0.3 mm) and 4 (colorless; 0.4 × 0.25 × 0.15 mm) were mounted on an Enraf-Nonius CAD4 diffractometer. The crystal data and data collection parameters are summarized in Table III. The unit cells were determined and refined from 25 randomly selected reflections obtained by use of the CAD4 automatic routines. Intensities were corrected for Lorentz and polarization effects, and an empirical absorption correction was made for 3. The Enraf-Nonius SPD library[25] was used for data reductions, and the solution and refinement of both structures were performed with SHELX76 programs.[26] Neutral-atom scattering factors and anomalous dispersion corrections were those given by Cromer and Waber.[27] The structures were solved and refined by conventional three-dimensional Patterson, difference Fourier, and full-matrix least-squares methods. All non-hydrogen atoms in the cations of 3 and 4 were refined with anisotropic temperature factors, but isotropic factors were applied to the atoms in the BF$_4^-$ anions. All hydrogen atoms were placed in calculated positions riding on the carbon atoms bearing them and included in the final calculations with B_{iso} fixed at the values equal to 1.3B_{eq} for the corresponding carbon atoms. The BF$_4^-$ anions in both structures exhibit a similar kind of disorder concerning three of the four fluorine atoms. These atoms were refined with occupancies equal to 0.5. Final positional parameters of non-hydrogen atoms are given in Tables IV and V for 3 and 4, respectively.

Acknowledgment. We gratefully acknowledge financial support from the Dirección General de Investigación Científica y Técnica (DGICYT; Grant No. PB89-0206) of Spain. We thank M. T. Compain for her technical assistance.

Supplementary Material Available: Tables of anisotropic thermal parameters, hydrogen atom coordinates, all bond distances and angles, and least-squares planes for complexes 3 and 4 (12 pages). Ordering information is given on any current masthead page.

OM920340W

---

(25) Frenz, B. A. The Enraf-Nonius CAD4-SDP. A Real Time System for Concurrent X-ray Data Collection and Crystal Structure Determination. In *Computing in Crystallography*; Schenk, M., Olthof-Hazekamp, R., Van Koningsveld, M., Eds.; Delft University Press: Delft, Holland, 1978.

(26) Sheldrick, G. M. SHELX76; University of Cambridge, Cambridge, England, 1976.

(27) Cromer, D. T.; Waber, J. T. *International Tables for X-ray Crystallography*; Kynoch Press: Birmingham, England, 1975; Vol. IV.